

See discussions, stats, and author profiles for this publication at: <https://www.researchgate.net/publication/268559718>

Mission Trade-Off Analysis of the Italian USV Re-Entry Flying Test Bed

Conference Paper · November 2006

DOI: 10.2514/6.2006-8017

CITATIONS

23

READS

1,480

9 authors, including:



E. Filippone

CIRA Centro Italiano Ricerche Aerospaziali

61 PUBLICATIONS 298 CITATIONS

SEE PROFILE



Giuseppe Mingione

CIRA Centro Italiano Ricerche Aerospaziali

41 PUBLICATIONS 383 CITATIONS

SEE PROFILE



Giuseppe Pezzella

University of Campania "Luigi Vanvitelli"

185 PUBLICATIONS 1,381 CITATIONS

SEE PROFILE



Vito Salvatore

CIRA Centro Italiano Ricerche Aerospaziali

45 PUBLICATIONS 319 CITATIONS

SEE PROFILE

Mission Trade-off Analysis of the Italian USV Re-entry Flying Test Bed

A. Schettino, E. Filippone, G. Mingione, G. Pezzella, M. Solazzo, V. Salvatore and P. de Matteis
Centro Italiano Ricerche Aerospaziali, Capua 81043 Italy

E. Bertuccio and F. Massobrio
Alcatel Alenia Space Italia, Strada Antica di Collegno 253, Torino 10146 Italy

The results of the ongoing trade-off and design activities in the framework of the USV Italian Space Program, addressed to the identification of the best suited aerodynamic and thermal design of the FTB-X in-flight demonstrator, are presented. The selected concept and the architectural design respond to the in-flight testing, performance and mission requirements set up at the beginning of the study, as part of the USV overall experimental logic for the validation of enabling technologies for future re-entry vehicles.

Nomenclature

<i>FTB</i>	=	Flight Test Bed
<i>USV</i>	=	Unmanned Space Vehicle
<i>ORT</i>	=	Orbital Flight Test
<i>SRT</i>	=	Sub-Orbital Flight Test
<i>L</i>	=	Lift
<i>D</i>	=	Drag
<i>W</i>	=	Weight
<i>UHTC</i>	=	Ultra High Temperature Ceramics
<i>S_r</i>	=	Reference surface
<i>LV</i>	=	Launch Vehicle
α	=	angle of attack
β	=	sideslip angle
C_L	=	lift coefficient
C_n	=	sideslip moment coefficient
C_m	=	pitch moment coefficient
<i>CoM</i>	=	Centre of Mass
<i>RCS</i>	=	Reaction Control System
<i>AoA</i>	=	Angle of Attack
<i>CSG</i>	=	Guyana Space Center
<i>P/L</i>	=	Payload
<i>AVUM</i>	=	Attitud and Vernier Upper Modules
<i>TVC</i>	=	Thrust Vector Control

I. Introduction

In the framework of the USV program, carried out within the Italian Aerospace Research Program (PRORA), a trade-off analysis is going on aimed at defining the configuration and the mission profile of a future experimental Flight Test Bed, called FTB-X, devoted to re-entry flight experiments. Such vehicle will be launched by the Italian launcher Vega and re-enter the earth atmosphere, thus allowing performing a number of experiments on critical re-entry technologies. Different challenging performance, design and technology validation requirements shall be fulfilled by the selected vehicle configuration and functional architecture. In particular, FTB-X shall exhibit well improved stability (aerodynamic) and maneuverability characteristics, allowing performing long endurance re-entry patterns, beyond one hour, as compared to conventional lifting re-entry vehicles¹.

It is worth to remind that a first version FTB's family, namely FTB-1 and FTB-2 (that differ only for the ventral fins that were adopted in FTB-1), designed to perform a number of flights in transonic and low supersonic regime, is about to be launched at the end of 2006, by means of a stratospheric balloon. This FTB-1 configuration² represents the basis for the current design activities on the FTB-X vehicle, with the major constraint to allocate such a vehicle in the fairing of Vega launcher.

II. USV_X mission: definition and requirements

Two types of missions have been identified within the re-entry flight mission envelope of the USV program.

Orbital Re-entry Test (ORT)

This mission shall be considered as the reference mission of the FTB_X vehicle. It shall consist of a complete re-entry flight from LEO orbit at 200 Km (to be confirmed by the launcher capability). An improved gliding re-entry and a high maneuvering capability, as compared to the reference re-entry vehicle Space Shuttle, characterized by moderate angle of attacks (down to and below than 20°) and a longer flight duration shall be developed in order to allow for more extended in-flight testing capabilities in high energy hypersonic flight conditions.

The LEO orbit inclination as well as the landing site and the re-entry trajectory footprint shall be suitably selected, in order to fulfill the safety requirements for ground population as per later requirement.

Sub-orbital Re-entry Test (SRT)

This type of mission of the FTB_X vehicle may be envisaged in the mission plan as an intermediate step for both design validation and risk mitigation purposes. Indeed, the mission plan shall be conceived in order to gradually achieve the ORT reference mission capability, as above defined.

Design Requirements

Aerodynamic Shape	Wing-body configuration with: - improved (L/D) ratio, up to a maximum value of [2-2.5] at Mach number in the range [8-10]; - reduced (W/Sr) down to 100 Kg/m ² ; - as compared with reference lifting re-entry vehicles
Primary Structure	Based on a lightweight design approach to comply with reduced (W/S) requirement. Compliant with the most critical static and dynamic thermo-mechanical loads identified in the various mission phases. Compatible with novel hot structures concepts based on advanced UHTC materials, either complete vehicle sub-assemblies (nose cap and wing leading edge) or embedded material samples. Allowing integration of payloads according to the in-flight testing needs.
Thermal Protection System	Compliant with aero-thermal loads experienced during the atmospheric re-entry (up to 25 MJ/KG) and extended re-entry. Design compatible with hot structures based on UHTC massive ceramics on the mostly exposed parts of the vehicle Design to minimize abrupt steps and gaps along the outer mould line within acceptable limits to avoid heat peaks.
Guidance, Navigation and Control	Provide autonomous on-board attitude and flight control capabilities in the overall re-entry phase, either using a reaction control system or aerodynamic control surfaces. Handle large aerodynamic uncertainties and a wide Mach number range, from hypersonic to low subsonic as well as a defined set of off-nominal conditions (robust design).
Avionic System	Main functions to be provided: i) on-board Data Handling, for both housekeeping and scientific data; ii) Telemetry Tracking & Communications; iii) up-link and down-link functionalities to be properly defined; iv) electrical Power provision for all subsystems for long mission. Qualification defined according to applicable standards for the above defined space and re-entry missions. Designed to be reconfigurable for different missions and experiments

Instrumentation	Housekeeping instrumentation, for flight parameters acquisition and any system monitoring function; Scientific sensors, as resulting from in-flight experimentation requirements and related design activities. Accommodation of a dedicated bay for self-standing passenger experiments (e.g. microgravity) to be investigated.
Launch System	ORT to be accomplished with the VEGA launcher, possibly using the AVUM fourth stage for orbit injection, orbiting and de-orbiting. SRT to be accomplished either with the VEGA launcher or other available launcher or booster compatible with the vehicle design.
Landing and Recovery	The vehicle shall be landed in the sea after a final parachuted descent phase. Location site to be selected according to the following factors: i) minimum time of recovery of the vehicle, in any case lower than 48 hours (TBC); ii) applicable aero-navigability regulations during the final descent and parachuted phase; iii) need of a logistic base to support the operations in the proximity of the recovery area.
Life cycle and turn-around	Each unit of the FTB_X vehicle shall be capable of performing more than one flight, either sub-orbital or orbital, with a target of 5 flights. After mission completion, the vehicle shall be made ready to operate in 12 months (TBC), after proper refurbishment and reconfiguration according to the new mission requirements.

III. System design and verification loop

A. Approach to configuration generation

The FTB_X aerospace laboratory will be a single payload for the VEGA Launcher; consequently its envelope dimensions are strictly defined by the full usable dynamic volume of the VEGA fairing ($\emptyset=2.3$ [m], Length=5515³ - 6300⁴ [mm]), and with the spacecraft mass and CoM position that shall be compliant with a limitation for static moment applied to adapter interface. The adapter 937B is the current baseline.

All preliminary analyzed configurations have been obtained as combination of three main parts: wing, fuselage and tail. For each of them, a restricted number of concepts (e.g. single or double tail) and of geometric parameters have been adopted to create various vehicle external shapes. The "FTB-X Model" has been built up using a CAD Program (CATIA 5 version R12) with IGES format for the output files. The CAD model relevant to the fuselage portion has been created parametrically, while, actually, the wings and the tails components in the models are not parametric because related to the constant data-points used to describe the sections profiles.

The trade-off configurations analysis has been performed adopting a homogeneous set of independent parameters and of performance and/or merit indexes related to the requested functions, using the FTB_2 shape architecture as starting point.

The CAD outputs have been supplied to the involved design disciplines (e.g. aerothermodynamics, internal configuration, thermal protection, cold structures, power management, mission analysis) to work with an integrated approach on the same configurations database.

Dedicated tools have been created to perform sensitivity analysis about the different configurations that, at system level, support the trade off task, adopting several different performance indexes.

The external shapes have been described by means of suitable surfaces; the continuity of such surfaces and of the first derivative is guaranteed, except for junctions. Therefore the CAD model is not only able to give input to the preliminary aero-thermodynamic analysis, but also to more sophisticated CFD approaches.

This approach allows generating, on demand, a new configuration (having the same topological characteristics) with associated preliminary descriptive documentation (e.g. Drawings) in about 4 hours. In any case, no fillets were, in this preliminary phase, adopted between the fuselage walls and the wings, as well as for the tail, to assure a fast reactive process. Their implementation shall be performed in a next phase.

B. Aerodynamic Analysis

Project requirements influence:

The project requirements that drive the aerodynamic design are recalled, and the main impacts of each requirement on the aerodynamic configuration are emphasized.

Requirement 1: **High maneuverability**

The main consequence of this requirement is that the vehicle has to be design balancing the normal need to have a good stability with the possibility to perform the maneuvers that will be defined by the payloads and by the System itself. In fact it is known that if a vehicle is too stable, it is characterized by a lower capability to maneuver. This

aspect must be taken into account in the definition of the wing position and of the control surface, in strong synergy with the flight mechanics analysis.

Requirement 2: Capability to manage long missions, from 1 to 3 hours

This requirement has a major impact on the sizing of the TPS; however, a long mission implies also the need to minimize as much as possible the heat loads all over a vehicle.

Requirement 3: Moderate angles of attack with respect to Shuttle

The requirement to have a moderate angle of attack is mainly related to the request to fly at high efficiency (see requirement 6). The heat flux distribution will obviously be strongly influenced by the angle of attack, being in general the heat load on the wind-side lower with respect to the one that would occur at 40 degrees of AoA (typical of the Shuttle); on the other hand, the heat flux on the lee-side will be higher due to the lower expansion.

Requirement 4: Winged vehicle and similarity with FTB-1

This requirement is very challenging, also considering the constraint in the maximum wing span due to the use of VEGA launcher (see requirement 8). The only way to realize a wing span at least equal to the one of FTB-1 would be to strongly reduce the dimension of USV; on the other hand, this would be in contrast with the need to have a sufficient volume to allocate both the payloads and the tanks for the stability control.

Requirement 6: Higher efficiency with respect to Shuttle

In order to realize the required high efficiency, it was necessary on one side to guarantee a good slenderness of the vehicle, and on the other side to fly at moderate angles of attack (see requirement 3).

Requirement 7: Low wing load W/Sr

In order to fulfill this requirement, the wing surface was increased, by increasing the chord of the wing, in order to balance the reduction of the wing span. However, it must be noted that for a hypersonic re-entry vehicle the most appropriate reference area to be used is the plan form surface, rather than the wing, because a higher contribution to the lift coefficients comes from the fuselage.

Requirement 8: Use of VEGA launcher

This requirement has a strong impact on

- the overall dimension of the vehicle
- the maximum wing span
- the height of the fin

Aerodynamic configurations improvement

The aerodynamic analysis was performed for all the configurations with simplified tools, while CFD computations have been used in this phase only to have a preliminary estimate of the errors.

The Mach range 2÷25 was analyzed for several candidate configurations, with the goal to provide the aerodynamic coefficients for the trajectory analysis. The behavior at lower Mach numbers will be analyzed in more detail in the future; however, it must be underlined that, due to the fact that the FTB-X configuration is derived from the FTB-1, it can be expected that the behavior in low speed regimes will be comparable to the one of FTB-1, apart from the effect of ventral fins. Moreover, important information will be obtained by the first flight of FTB-1.

The aerodynamic coefficients have been provided as a function of Mach number (2÷25), Reynolds number ($2 \cdot 10^4 \div 2 \cdot 10^6$), angle of attack α ($0^\circ \div 30^\circ$) and sideslip angle β ($0^\circ \div 8^\circ$).

Also the heat loads were estimated for a number of selected points along the trajectories. The details of the aerothermodynamic analysis are described in ³.

For the last configuration (FTB-X_392-FW50) also the wing flaps deflections have been considered ($-10^\circ \div 30^\circ$), while the body flap effect has not been directly taken into account so far.

In the present paper only continuum regime (supersonic, and hypersonic speed ranges) results are shown, but a preliminary analysis has been performed also taking into account rarefaction effects.

For all the configurations, the following reference parameters have been chosen:

- $L_{ref} = 2.30$ [m] (wing mean chord of FTB-X_1.1.1)
- $S_{ref} = 3.05$ [m²] (area of the exposed part of the wing)
- Pole coordinates are (3.113, 0, 0) [m] (preliminary CoM).

It must be noted that, as heritage of the FTB-1 vehicle data base, the area of the exposed part of the wing was chosen as reference rather than the most suitable global plan form area.

In the present paper only the main configurations that were analyzed are described, emphasizing the rationale for each proposed change.

In the next figure the main configurations recalled hereinafter are shown.

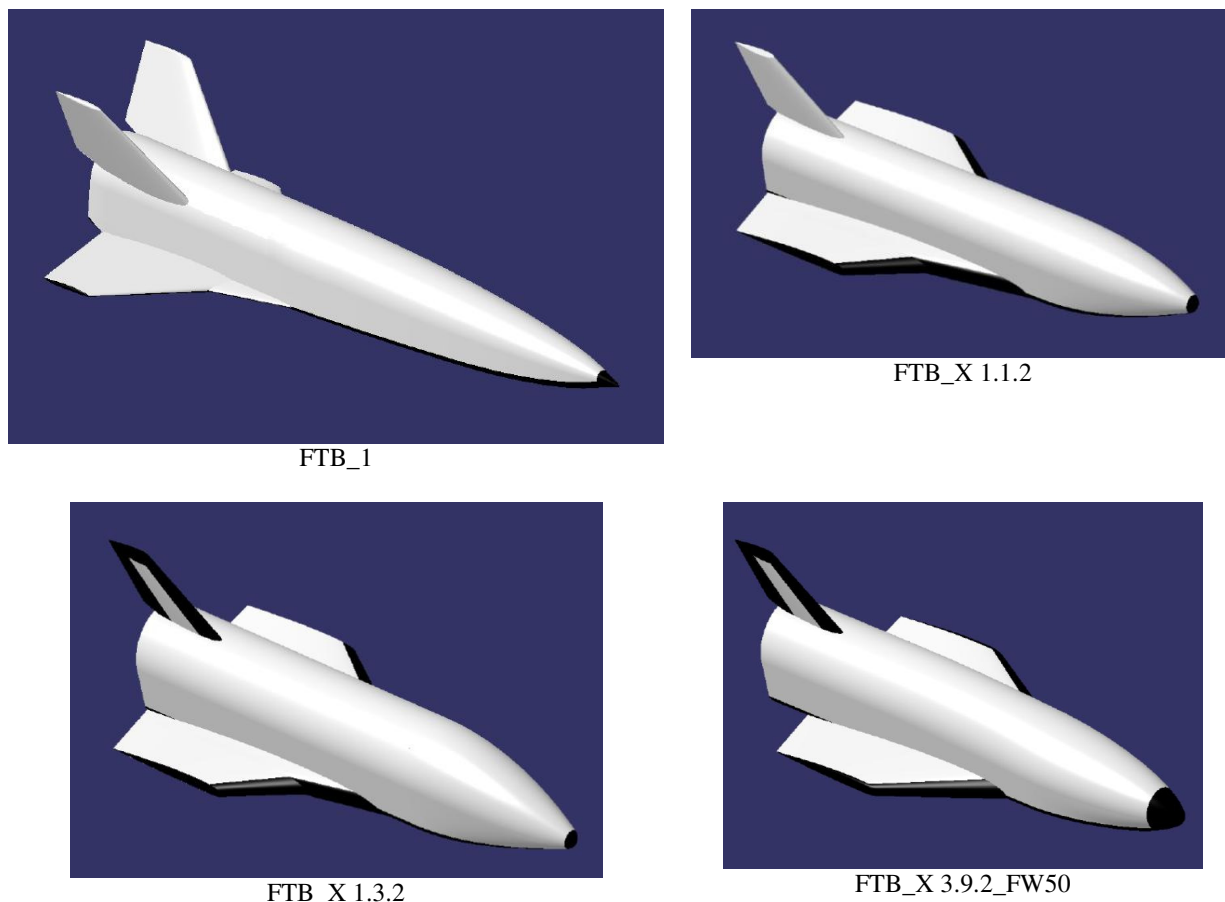


Figure 1 FTB_X main configurations (FTB-1 is not to scale; FTB-1 length = 8 m, FTB-x length = 5.310 m)

A preliminary FTB-X configuration, named FTB-X_1.1.1, was initially generated by scaling FTB-1 of about 65 % and shortening the forward part of the fuselage, with the aim to make it compatible with the fairing of VEGA launcher, maintaining adequate available vehicle inner volume to allocate subsystems. Since with such scaling the wings tips resulted out of the fairing, they were cut; however, the wing mean chord has been increased to compensate the area reduction in order to reduce the wing loading; the normalized wing profiles have not been modified to maintain similarity with FTB-1.

Moreover, the FTB-X_1.1.2 configuration was obtained simply substituting the double fin with a single one.

In order to optimize the heat flux distribution over the nose and to increase the vehicle aerodynamic efficiency, the vehicle forebody has been moved downward, obtaining a flat bottomed configuration, typical of winged hypersonic vehicles (FTB-X_1.2.2).

A further modification was required in order to increase the available volume; to this aim, the fuselage was laterally enlarged by 5 cm for each side (FTB-X_1.3.2).

Starting from the FTB-X_1.3.2 configuration, a sensitivity analysis was made with the goal to improve the longitudinal and lateral-directional stability, as well as the aerodynamic efficiency of the vehicle.

Several changes have been made also for the wing, with respect to the starting one, in terms of planform shape and of position with respect to the vehicle nose. The strake has been removed and the sweep angle has been increased from 60° to 65° (deg). The strake was removed because the one resulting from the scaling of FTB-1 toward the 1.1.2 configuration is no longer effective, and a detailed redesign would be needed; a newly designed strake could be added in the future, depending on the confirmation of a specific landing requirement.

A higher sweep angle, instead, was needed in order to increase both the efficiency and the wing area and to assure best performance with respect to the supersonic drag and aerodynamic heating.

The final important change consisted of moving the wing forward by 50cm (FTB-X_3.9.2-FW50), in order to increase the C_{m_y} and to allow to pitch trim the vehicle with positive deflections of control surfaces, so improving

the vehicle stability and controllability for major parts of the flight envelope; the final position of the wing will be however fixed after a further trade-off with the CoM position.

As far as the lateral-directional stability is concerned, it is well known that, using the standard aeronautical conventions, the $C_{n\beta}$ should be positive to guarantee the static stability; however, it is also known that for a Shuttle-like vehicle, at high Mach number, to obtain a positive $C_{n\beta}$ is almost impossible unless a very high dihedral angle is used for the wing (i.e. X-38). Therefore the use of lateral RCS must be foreseen for a large part of the trajectory. Nevertheless, a sensitivity analysis was deemed useful in order to increase the value of $C_{n\beta}$, so reducing the work of the RCS. For example, in the FTB-X_1.7.2 shape, the fuselage height was reduced by 10 cm, obtaining a significant increase of the $C_{n\beta}$. However, since in such way the available internal volume was also reduced, a different solution was proposed in configuration FTB-X_1.9.2, where the fuselage height was kept equal to the 1.3.2 from the 65% of the vehicle to the base, while is gradually reduced from 0.9 m to 0.8 m in the forward part.

In Figure 2 the $C_{n\beta}$ is shown for two angles of attack (15 and 30 deg) for different configurations at Mach 15; it can be clearly seen the improvement of the $C_{n\beta}$ up to the 1.9.2 configuration; unfortunately a decrease of $C_{n\beta}$ occurred for the 3.9.2-FW50 configuration, due to the fact that the wing has been moved forward by 50 cm.

In Figure 3 the evolution of the efficiency with the configurations is shown; it can be seen that, from the 1.1.2 to the 1.3.2 configuration, there have been a decrease of the efficiency, mainly due to the minor slenderness of FTB-X_1.3.2. Going to the 3.9.2-FW50 configuration, a positive trend was obtained and an efficiency closer to the fulfillment of the project requirements was accomplished.

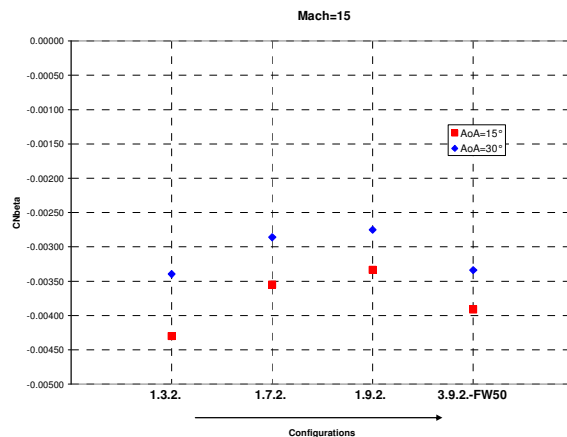


Figure 2 $C_{n\beta}$ vs. configurations

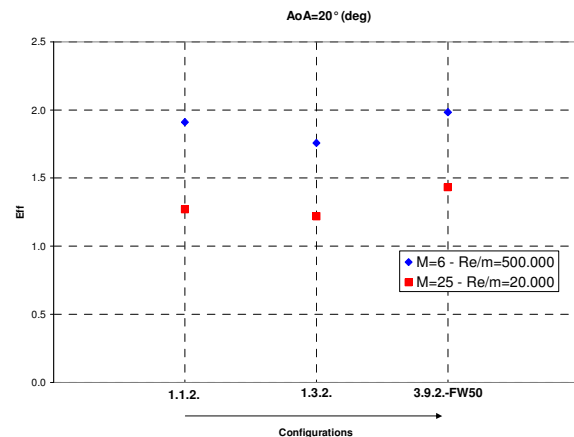


Figure 3 Efficiency vs. configurations.

Finally, in the Figure 4, the pitch moment coefficient is shown for three configurations; it can be clearly seen the effect of the configuration changes on the C_{m_y} .

In the following figures some of the main results obtained for configuration 3.9.2-FW50 are shown. In Figure 5 the estimated aerodynamic efficiency is plotted for 3 values of the Mach and Reynolds numbers, as a function of the angle of attack; in Figure 7 the pitch moment is shown for the same conditions. It can be seen that the vehicle is longitudinally stable with the given CoM (3.113 m from the nose) for angles of attack higher than 15 degrees, and being the C_{m_y} positive and sufficiently small, it can be trimmed with positive deflections of the control surfaces.

In order to provide data for the trim and stability analysis, a preliminary hypothesis was made for the control surfaces. In this phase only the wing flaps have been taken into account; the flaps efficiency is shown in Figure 6. By comparing the flap efficiency with the C_{m_y} shown in Figure 7 it can be clearly seen that a deflection between 10 and 15 degrees is sufficient to longitudinally trim the vehicle. In the next section a more detailed trim analysis is shown; on the basis of such analysis, the next step will be to define a suitable dimension and position for the body flap and to refine the design of the wing flaps.

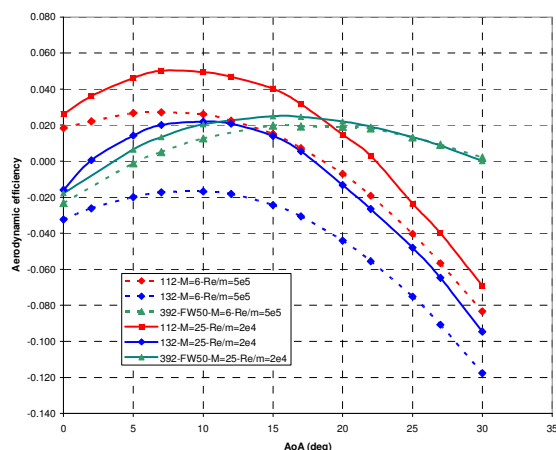


Figure 4 Pitch moment coefficient vs. configurations

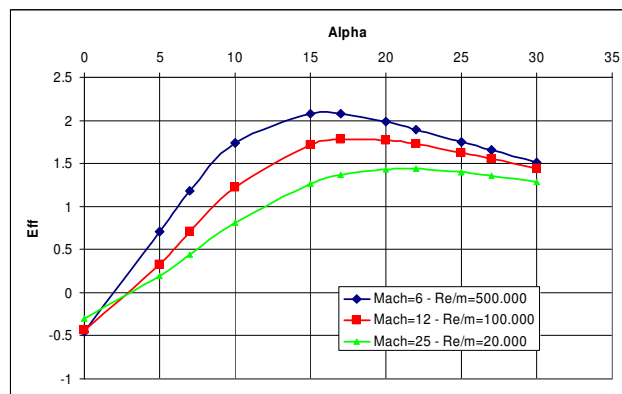


Figure 5 FTB-X_392-FW. Aerodynamic efficiency.

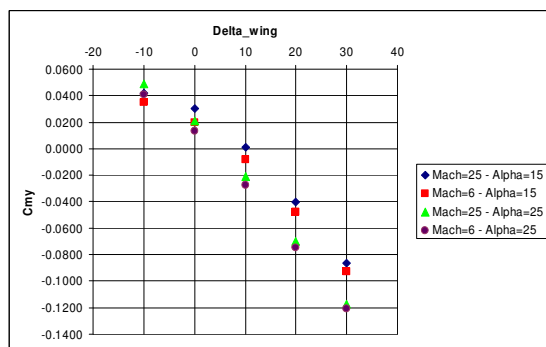


Figure 6 FTB-X_392-FW. Wing flaps efficiency.

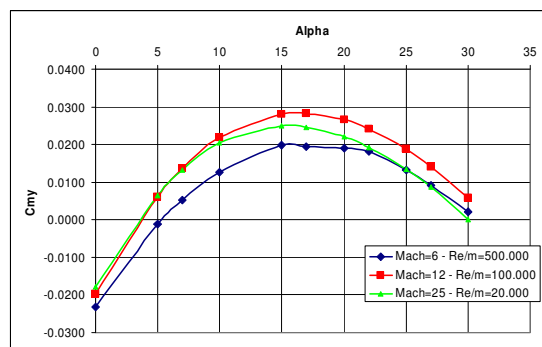


Figure 7 FTB-X_392-FW. Pitch moment coefficient.

C. Flight Mechanics

The re-entry mission analysis is performed, with reference to the configuration under analysis, using the point-mass aerodataset (C_L - C_D coefficients as a function of Mach, AoA and Reynolds number).

Due to peculiarity of mission requirements, the guidance strategy adopted aims to test the AoA modularity, in a re-entry mission that it is foreseen to be flown entirely in a local vertical plane, thus nominally involving just the vehicle longitudinal dynamics, to which the analyses are referred.

Re-entry mission analysis

The reference initial conditions (i.e., the vehicle dynamical status at the entry interface) has been generalized to a set of five, to widen the admissible vehicle release conditions that had to be generated by the Vega launcher.

The nominal vehicle dataset is characterized by the following values:

Vehicle length (l)	5.310 [m]
Vehicle mass (m)	1034.4 [kg]
Reference Aerodynamic Area (S)	3.05 [m ²]

Table 1 nominal vehicle data

The basic mission requirement of performing a re-entry modulating the angle of attack (instead of the bank angle as usually done in re-entry guidance profiles), has been assumed in mission and trajectory optimization.

The strategy adopted in the orbital re-entry mission of the FTB_X is to modulate the AoA profile during entry critical phases, taking the angle of attack as close as possible to that corresponding to the maximum efficiency (at

least in the “dense” atmosphere range), compatibly with the maximum heat flux that the vehicle (TPS and structure) could sustain. This kind of AoA guidance profile should be beneficial for a number of factors, such as to have a greater vehicle manoeuvrability along the trajectory and to expose a smaller part of the vehicle to the higher heat flux, then allowing a TPS mass reduction and increasing the mission safety level.

In the following Figure 8 the results are reported of the trajectory optimization, performed assuming this strategy for the re-entry guidance, with reference to one of the five analysed different initial conditions at entry interface.

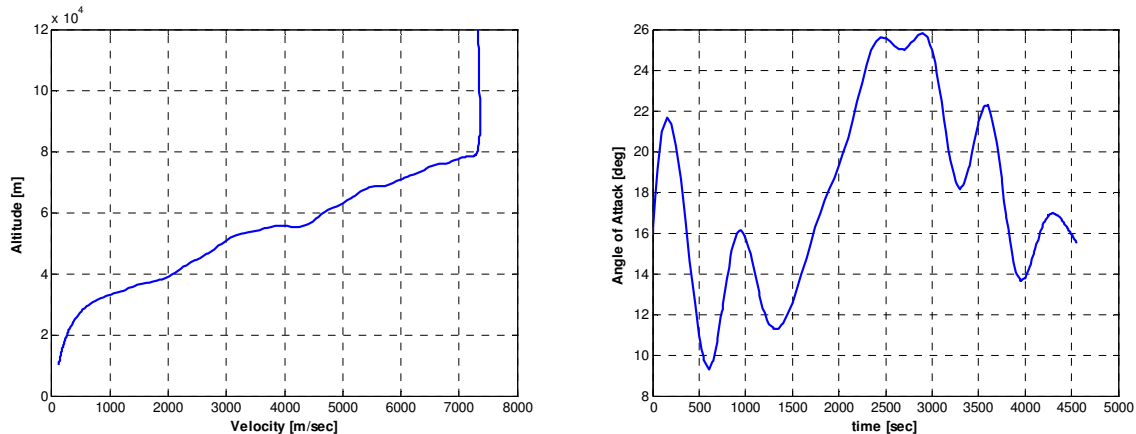


Figure 8 Trajectory path and Angle of Attack guidance law for FTB_X re-entry mission

Actually, for all such initial conditions, the reference trajectories are quite similar, and just small changes in the AoA guidance profile are required to generate the different paths in correspondence of the different conditions at atmosphere entry point (conventionally chosen at 120 km of altitude). Depending on which of the studied conditions will be better realised by the carrier (Vega Launcher), the reference trajectory for the orbital re-entry mission will be identified in detail.

Trim maps and stability properties

Trim maps of the aerodatabase, once translated to the nominal CoM position, were realized at different Reynolds numbers; however the differences between such trim maps are very small, and actually very subtle between the two trim maps corresponding to the two major Reynolds numbers for which the aerodatabase has been provided. Therefore in Figure 9 only the trim map corresponding to Re/m 500.000 [1/m] is reported.

In any case, also in the most demanding flight condition, corresponding to hypersonic Mach numbers (10 to 25) and AoA in the range $10 \div 15$, no more than 15 degrees of elevon deflection are required to achieve the vehicle trim

condition, and wide margins of elevon deflection are left for the vehicle controllability.

At low supersonic Mach number, instead, the elevon deflections required to trim the vehicle invert the sign and the vehicle becomes quickly untrimmable, at least for the available range of data, which reduces to only 10 deg for negative deflections.

To appreciate stability properties of the vehicle, in a preliminary evaluation, the pitch moment coefficient behavior with AoA can be analyzed, stating that the aerodynamic characteristics of longitudinal stability are mainly expressible through the Cm_a derivative.

The Cm_y behavior is described in the

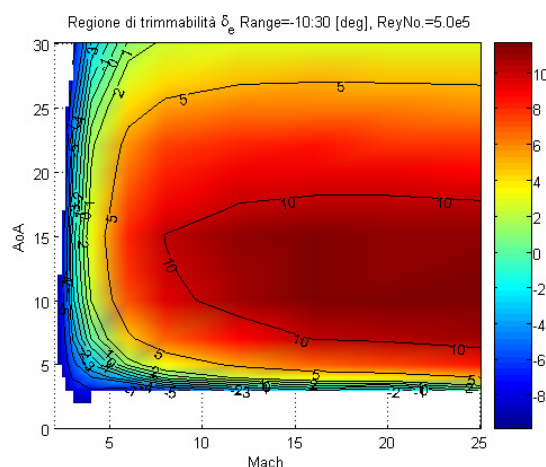


Figure 9 Trim Map

following Figure 10, for a number of Mach and Reynolds numbers representative of all the Mach and Reynolds range, and for all the admissible elevon deflections.

The figures show that the vehicle can exhibit instabilities for AoA under 10 degrees, while the vehicle behaviour seems to be aerodynamically stable for all the AoA values greater than 20 deg, for all Mach numbers and elevon deflections. Taking into account that the guidance strategy requires the AoA modulation, it can then be expected that instabilities can arise along the reference trajectories for the current configuration. The level of these instabilities will be evaluated in the following.

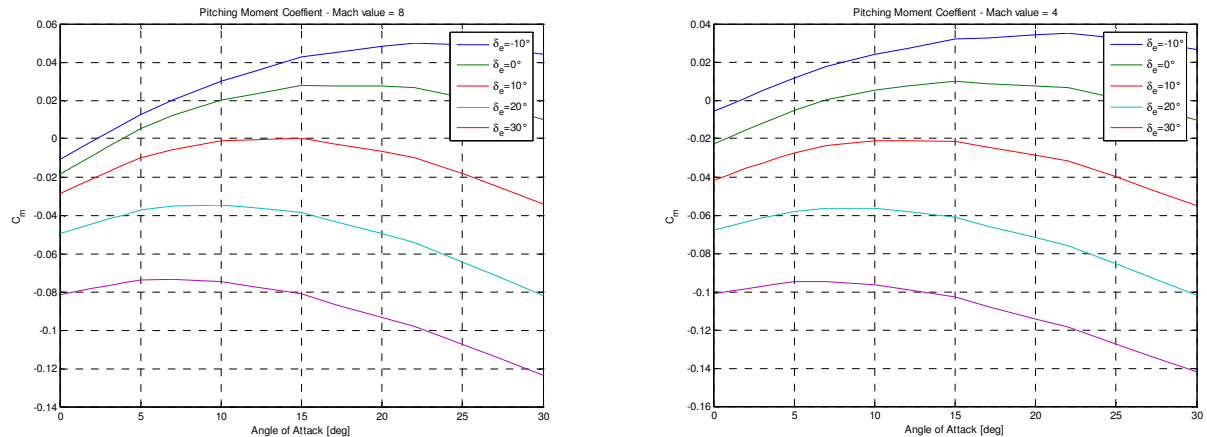


Figure 10 Pitch moment coefficients. Mach=4, Mach=8

Stability and maneuverability properties

With reference to the trajectories considered, three measures will be provided of the margins presently existing on maneuverability and stability behavior of the vehicle, i.e. a) the Maneuverability Margins, described by the margins between the trimming elevon deflections and the relative maximum deflections, b) the Static Margin, described in terms of normalized coordinate of the Neutral Point and approximated by the ratio $-Cm_q/C_{L\alpha}$, and c) finally, the CoM displacement limits at the maximum elevon deflections.

Analysis of Figure 11 highlights that, for the present CoM nominal position, the elevons deflections required to trim the vehicle along both the considered trajectories are well under the 50% of all the admissible deflections, but in short trajectories pieces at about the beginning and the end of the re-entry phase.

The reduction in maneuverability experimented in the first part of re-entry, particularly evident for some of the analyzed trajectories, is not actually of concern. In the associated flight conditions, in fact, the dynamic pressure is too low to allow the vehicle to be governed by the aerodynamic surfaces alone, and RCS is required to command vehicle attitude changes and trim attainment.

As far as the loss of trimmability at the end of the trajectories is concerned, these results in a problem that has to be more attentively analyzed.

At the moment, trim capabilities are known, for negative deflection of elevons, only in the range by 0 deg through -10 deg. If trimmability loss, at any AoA value and for any Reynolds Number, is confirmed also for the total admissible negative deflection range of elevons, a high critical condition can arise when flying in the supersonic and low-supersonic Mach regimes.

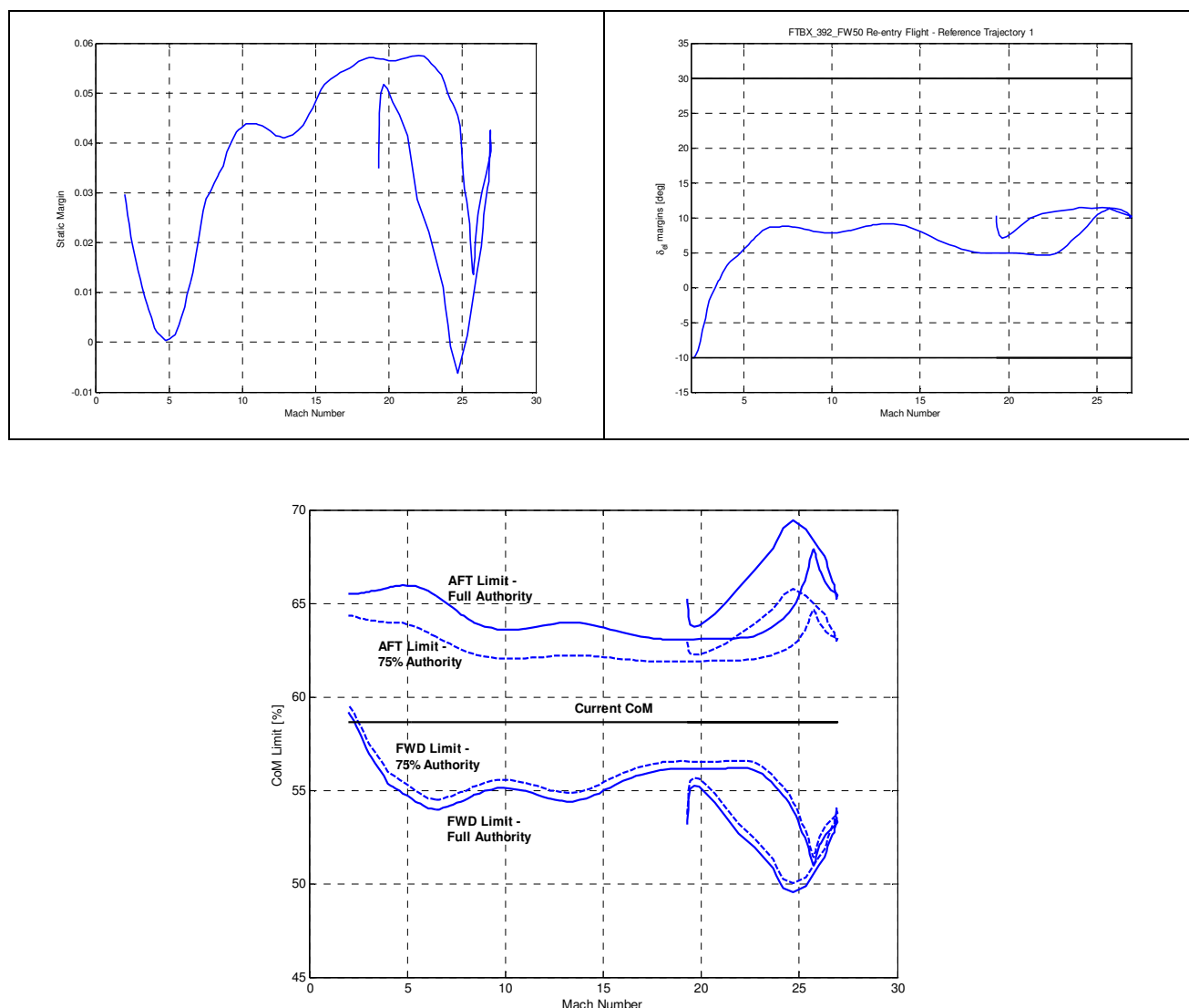


Figure 11 Stability and Maneuverability margins

A better measure of the stability behaviour of the vehicle along the reference trajectories is actually obtained by linearising the model of the vehicle dynamics at sampling flight conditions along the same trajectories.

The poles of the vehicle dynamics along the reference trajectory are provided in the following Figure 12, subdivided in time frames for readability reason.

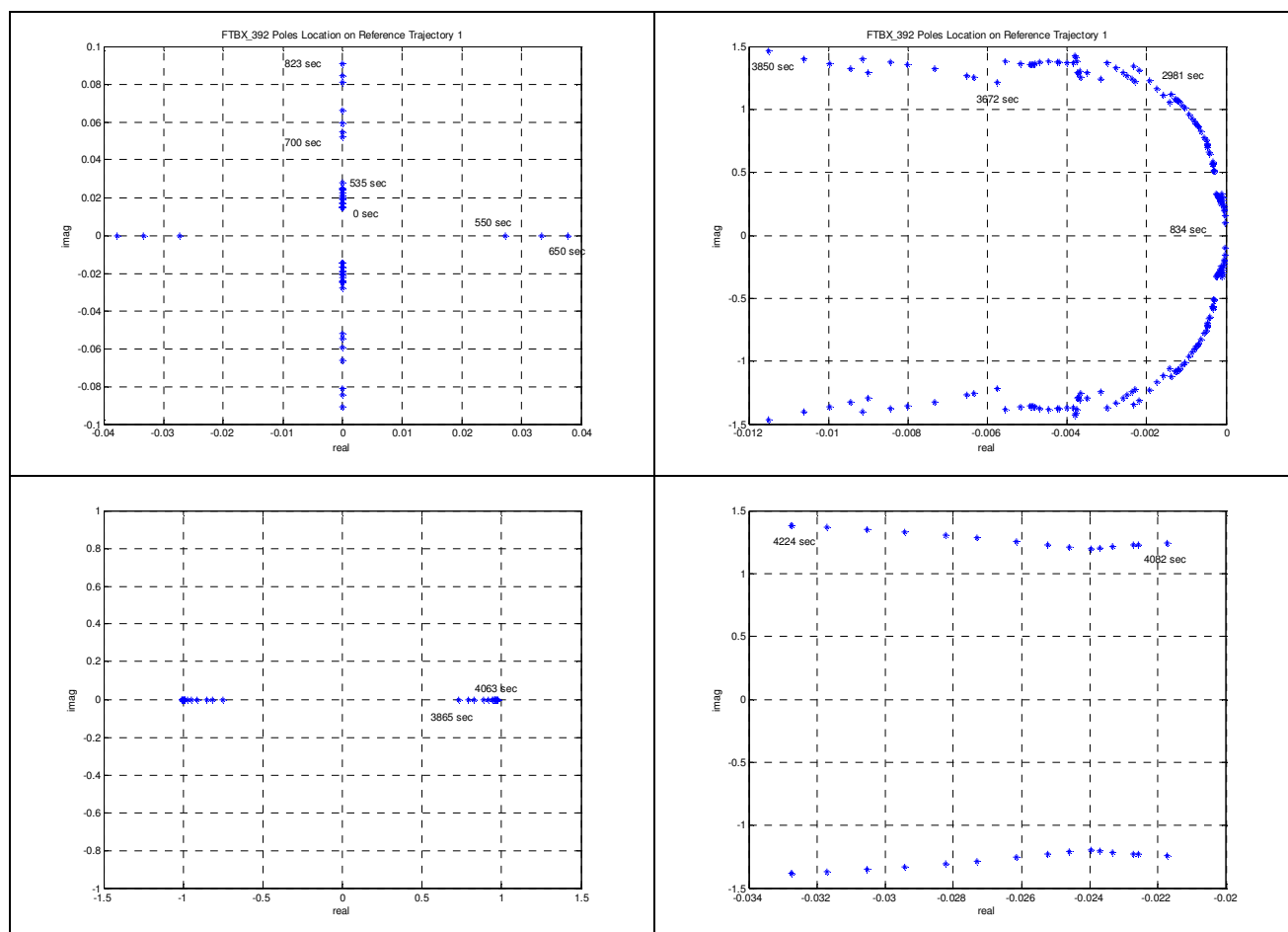


Figure 12 Poles map

The instabilities that arise at the end of trajectories are not of concern. In fact, these are mainly due to guidance law at relatively low AoA. Because in this phase the thermal and structural criticalities are not still a concern, we can easily maneuver in such a manner to avoid the instabilities that appear too strong to be recovered by the flight control system. The choice of the exact guidance law in this phase will be designed according to specific mission requirements not yet identified.

As far as the instabilities arising during the first re-entry phases, those seem not represent an actual critical condition for the trajectory analyzed in the figures above; in fact they are associated with a minimum time-to-double greater than 20 sec.

More critical appears to be the instabilities, for these same phases of re-entry in some others of the analyzed trajectories, which in some case are associated with a time-to-double less than 1 sec. The RCS system and the flight control system operated through aero-surfaces shall be capable to recover these instabilities.

Sensitivity analysis

A number of changes are expected on relevant parameters nominal values, and a sensitivity study has been agreed to be suitable in terms of variation to the reference trajectories under parameter value changes.

The sensitivity under investigation refers to the following parameters and relative values:

- a change of 50 Kg on vehicle mass;
- the change of pitching inertia moment has been estimated in an 8%, as a consequence of a mass variation of 50 Kg;
- the effect of the CoM displacement till the 61% of the vehicle length.

Figure 13 reports the results obtained in terms of nominal trajectory variations. It can be seen that a maximum increment of about 1.5 degree has been required in the most critical phase of the re-entry trajectories to reproduce almost exactly the correspondent reference trajectory for the vehicle with an improved 50 Kg mass due to a payload.

Due to the small changes required in AoA and elevon deflections for trim, it is reasonable to consider that only very limited changes can produce on the manoeuvrability margins and on the CoM shifting limits.

As far as the stability considerations are concerned, an improved vehicle mass can produce some change. These changes are, in any case, more sensible to inertia properties changes, that have, on the contrary, very little effect on the reference trajectories.

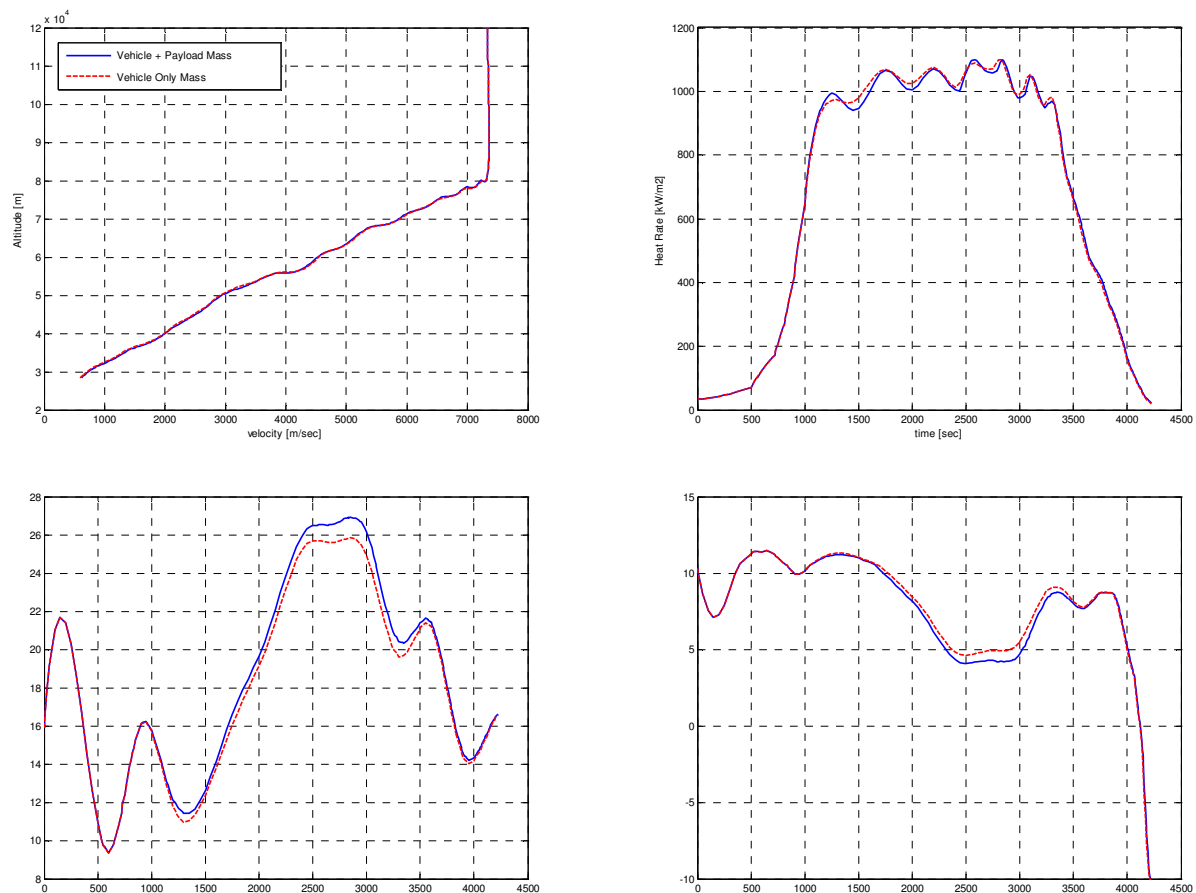


Figure 13 Trajectory changes under sensitivity analysis

Much more relevant are changes due to CoM displacement. In particular, for a backward displacement of the CoM till the 61% of the vehicle length the vehicle exhibit a loss of manoeuvrability in high Mach regimes, showing a decrease of deflections margins from about 60% to about 40%, but the same manoeuvrability property benefits at low Mach regime, where the criticalities that arose in the nominal CoM position, seems now to be lowered or disappeared. However, on the other hand, instabilities along the reference trajectories greatly worsen, and at least one pure real instable pole is now present all along the trajectory. Then, if required, a shift-back of the CoM position shall be attentively evaluated from a stability point of view.

IV. System Architecture

A. Thermo-mechanical configuration and structural layout

The internal structural concept of the vehicle is shown in the following figure.

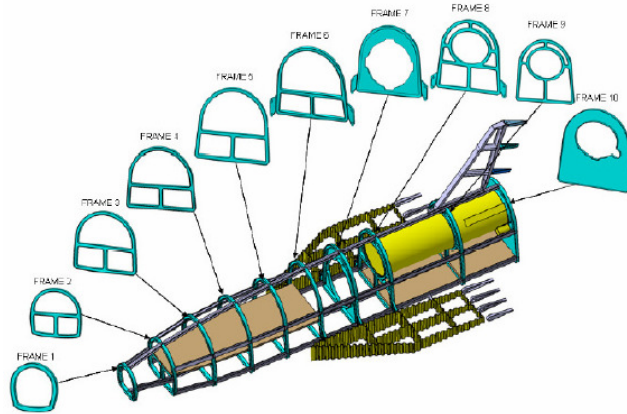


Figure 14 Structural concept

Basically, the structural architecture is composed by ten bulkheads connected by six longerons (“T” and “H” section) for each, of the nine subdivision of the external shell (the only exception is between the first bulkhead and the second one in the nose area where the longerons are only four); from the first one, in the nose, up to bulkhead mounted in the rear part of the vehicle.

The bulkheads are constituted by machined titanium plates that allow the accommodation of the parachute canister and the propellant tank.

Waffle architecture has been chosen for the rear bulkhead providing a stiff interface for the parachute canister mounting flange and for the attachments to the launch adapter.

The wings are conceived as hot structures in order to minimise the mass and to enhance the technological valence of the vehicle itself. The technologies so far considered are straightforward coming from the ASA program, intended as a USV-FTBX trailblazer in which critical technologies will reach a level of confidence sufficient to allow their implementation into a flying vehicle.

The wing internal skeleton will comply with the thermal induced deformations of the leading edge as well as the ones of the leeward and windward skin, being all of them made with dissimilar materials, with highly different values of the thermal expansion coefficient, hence there will be the necessity of an hard skeleton able to maintain the structural integrity of the wings in all conditions but flexible enough to be compatible with the deformations of its various parts without losing the wings aerodynamic efficiency.

These performances are pursued with spars and ribs realised as wrinkled sheets (high bending stiffness but low longitudinal stiffness, for which the skin in-plane stiffness will dominate the overall wing behaviour).

The Maximum internal temperature of the wing will be limited to 400°C. This limitation is not due to structural reasons (the materials used could exceed such limits) but for functional reasons (feasibility of an affordable aileron command chain). Within the above mentioned limit the Ti-alloy could be a valid candidate for the wrinkle, although the PM1000 was considered into the mass budget for sake of structural safety, hence to provide the structure with some margin in front of possible non-nominal events such as the loss of small portion of the TPS function (this approach is considered applicable to an experimental vehicle such the USV, for which the mission envelope will be affected by serious contingencies).

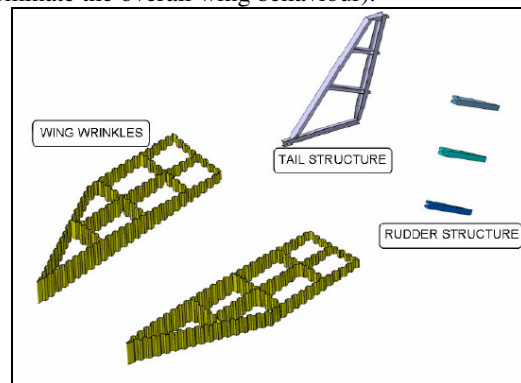


Figure 15 Wing concept

The wings are linked to the fuselage through a system of rods (so far considered in PM1000, but a Ni-based MMC is envisaged as an attractive potential substitute) enabling the transportation of fuselage and wings disassembled and then an easy re-assembly on the launch site facilities.

The Aileron is an integral C-SiC structure with embedded C-SiC stiffening. The selected solution is the best option both for the mass saving and for the thermal efficiency. Due to the high thermal conductivity of the C-SiC, the Aileron Hinges Bearings hosted into the wings will be in Ceramic (and their life will have to be checked in front of the missions to be performed by the USV, considering a possible bearings re-furbishing after a given number of missions).

The baselined wing leading edge is made of UHTC, but the wing will be able to host the fluidic distribution lines in case an actively cooled leading edge is chosen (depending from the ASA on going qualification activities outcomes).

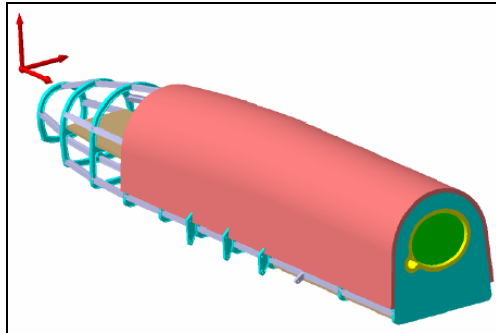


Figure 16 Fuselage concept

Inside the primary structure the vehicle electrical components are installed on three different panels as shown in the following figures. The tank is positioned in the middle of the seventh bulkhead

located approximately in the vehicle center of gravity. On the external side of the rear bulkhead the RSC thruster pods have been located, while the four EMA for the elevons, body flaps and rudder are situated immediately inside the vehicle internal volume. The four EMA are positioned in proximity of the flap and rudder rotation axis. The connection to launcher consists of four links located at the ending of longerons in correspondence of the connections to the rear bulkhead. The interface locations have been chosen because their positions are in correspondence of the main structural point at the rear side of the spacecraft.

The total length of the vehicle as well as the wing span is tuned to allow for a suitable accommodation inside the launcher fairing (nominally VEGA).

B. Thermal design

The energy management accomplishes two main functions:

- Protect the Kevlar primary structure from the severe aerothermal fluxes experienced especially during the re-entry phase;
- Ensure that the internal environment is maintained within the temperature limits suitable for the operative conditions of the avionics equipment, of the actuators and of the RCS tank.

The TPS layout has been conceived following the results of the preliminary thermal analysis with particular care of the selection of the associated technologies. Further results can be found in ³.

The subdivision of the TPS zones is reported in the following figure.

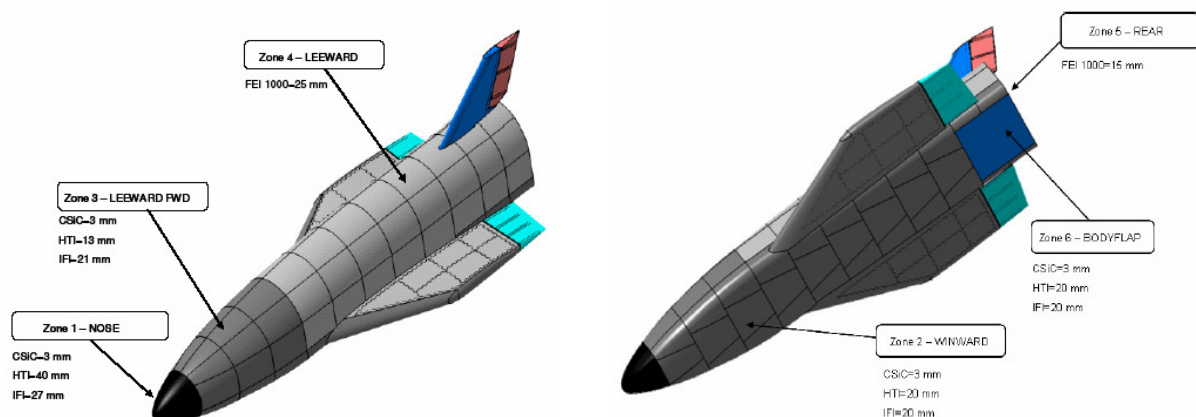


Figure 17 Thermal protection system layout

C. Avionic architecture

The avionics architecture is aimed to provide the necessary resources and functions to supply power to the system, to control and monitor the USV housekeeping data, to allow the trajectory reentry control and to support the payloads functions during the mission. The mission data (Housekeeping and payloads) will be recorded on board and transmitted to the Ground via a telemetry link. USV foresees a tele-command capability on-board in case of a

selected set of commands to be confirmed and defined in the next program phase. In general the mission is to be considered completely autonomous and it will be driven on the basis of pre-stored timeline and sequential key-events. Only a limited amount of automatic corrective actions in case of malfunctions can be considered at on-board level because the speed sequence of the mission events due the shortness of the mission (e.g. possible re-boot of the computer could not guarantee the successful recovery of the malfunction in time before an un-recoverable trajectory change). In order to increase the mission success criteria and the hazard safety the most critical functions have been redundant with a hot redundancy of the system. The not-critical functions are considered zero failure tolerant, so only minor failure may be recovered via software design robustness implementation.

It is clear that the total application of the redundancies could be guarantee higher reliability but it is not feasible in the USV because the mass and layout impacts due to the duplication of all the boxes can not be accommodate on the system.

The avionics architecture includes the following main functions:

- On-board Data Handling
- Electrical Power Supply, Distribution and Control.
- Communication and Tracking

In the following figure a typical Avionics Architecture and Instrumentation block diagram is represented.

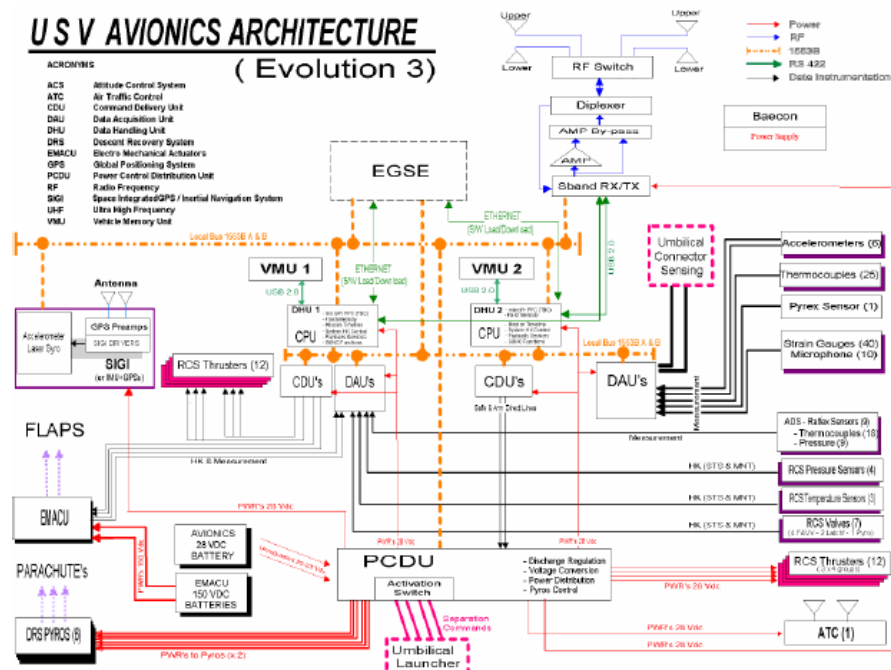


Figure 18 Typical avionics architecture

D. Re-entry Plasma Radio Frequency Blackout

When a spacecraft enters a planetary atmosphere at a velocity significantly exceeding the speed of sound, a shock layer forms in front of the body. The sheath of ionized particles, which develops around the spacecraft, is the result of ionization of the atmospheric gases as they are compressed and heated by the shock, or heated within the adjacent boundary layer.

When the electron density gets sufficiently high, such that it exceeds the critical plasma density of the link frequency, communications can be disrupted, with the result being significant attenuation or even blackout.

The main cause of blackout is reflection or absorption of electromagnetic energy at frequencies below the critical plasma frequency. At frequencies higher than the plasma frequency, the layer will be effectively transparent to the transmitted signal, and communications can take place.

A reliable prediction on the signal attenuation or blackout is in line with safety issues, in particular to avoid the blackout when populated zones are over flying.

Telemetry shall be recorded on-board during the expected blackout period and transmitted when communications are later restored.

The use of higher frequencies can reduce the blackout period or eliminate the blackout condition entirely.

The proposal, issued from the X-33 Program, consisting to place systems with higher gain antennas at the location where a signal attenuation or blackout is expected, is not feasible way for the USV Program.

V. USV_X VEGA compatibility analysis

A. Launch and de-orbit

Trajectory analysis was performed according to all the above mentioned constraints, for the whole LV mission (i.e. P/L separation after de-orbiting) and the descent phase until 120 km.

Table 2 provides the summary of the most relevant trajectory data⁴.

In particular, note that the fairing jettison is after 218.5 s, when the free-flow thermal flux is 860 W/m². After the jettison and up to the end of the de-orbiting firing, the P/L is exposed to a thermal load whose integral is 15.2 kJ/m².

In Table 3 the orbital elements at the key trajectory points are reported. The final entry conditions are matched, as the relative speed is 7420.1 m/s, and the flight path angle is 1.099°.

Figure 19 shows the trajectory ground track, together with the relevant TLM and tracking station available, together with their geometric horizon at the relevant LV altitudes. In particular, the sites marked with blue labels (Kourou, Libreville, Ascension, Malindi, and Biak – the last one TBC) are part of Arianespace network; the other ones, in red (Natal, Trivandrum, Pare Pare, Kwajalein), are known existing facilities which shall be fitted with a telemetry kit in order to be used, thus increasing logistic costs.

TRAJECTORY EVENTS					
STAGE/EVENT	TIME	REL.SP.	ALT.	WEIGHT	MACH
	[s]	[m/s]	[km]	[kg]	[-]
1 Mission St.	0.0	0.0	0.0	138124.1	0.0
1 Lift-Off	0.2	0.0	0.0	138083.3	0.0
1 Pitch-Over	3.7	29.4	0.1	134558.5	0.1
1 GravityTurn	18.9	204.5	1.8	118080.8	0.6
1 Mach 1	31.1	331.6	4.9	106921.6	1.0
1 P.dyn. max	52.0	554.5	12.7	90013.0	1.9
1 (T-D)/M max	93.0	1621.8	41.8	53824.4	5.0
1 Separation	108.9	1749.0	58.3	49551.5	5.4
2 Motor Start	109.5	1745.8	58.9	40936.2	5.4
2 (T-D)/M max	140.5	2632.3	93.5	28346.7	9.7
2 Separation	194.9	3854.7	173.5	16909.3	5.6
3 Motor Start	213.2	3791.3	199.8	14341.2	5.1
3 HS Jettison	218.5	3868.8	207.1	13882.7	5.1
3 (T-D)/M max	294.5	5997.8	276.8	5611.7	7.0
3 Separation	337.6	7136.8	283.4	3665.6	8.3
4 Motor Start	345.1	7136.5	283.6	2306.5	8.3
4 Cut-Off	488.0	7283.2	282.8	2193.4	8.5
4 Coasting					
4 Mtr Restart	2952.6	7188.6	360.1	2134.9	7.9
4 Cut-Off	2996.5	7201.3	361.2	2100.2	7.9
4 Coasting					
4 Deorbiting	3056.5	7201.4	361.1	2098.3	7.9
4 Cut-Off	3126.2	7119.3	360.9	2043.2	7.8

Table 2 ORT trajectory sequence

Orbital elements	3 rd stage	Transfer orbit (injection)	Transfer orbit (end of coasting)	Final	De-orbit	Re-entry (120 km)	
Perigee alt.	-100.880	274.002	287.194	360.998	79.905	64.734	[km]
Apogee alt.	285.649	399.496	385.795	361.001	360.919	377.228	[km]
RAAN ^(*)	-143.687	-143.689	-143.908	-143.994	-144.018	-144.138	[°]
Inclination	5.206	5.206	5.205	5.206	5.206	5.209	[°]
Perigee arg.	-70.012	141.763	156.373	-4.705	103.722	101.298	[°]
True anomaly	171.640	-30.682	118.713	-77.255	-177.208	-50.732	[°]

(*) For a launch at 0⁰⁰ UT.

Table 3 ORT: characteristic orbit elements

Figure 20 shows an approximate re-entry ground track. For all the ground stations along the flight path (Quito is added), the geometric horizon is plot for an altitude of 120 km, thus the useful one for tracking will be smaller (to be analyzed in the frame of USV re-entry trajectory analyses, out of the scope of the present document). Even though only a small part of the trajectory is deemed visible, Kourou, Libreville, and Malindi are in very good position along the flight path.

Additionally, when better accuracy will be provided for the landing location, an equipped ship for tracking and TLM (already available from Arianespace) could be placed in useful position.

For what concerns the LV mission feasibility, a significant reserve is available of about 260 kg of AVUM propellant (representing half its total load-out), which should grant a quite good margin for unexpected troubles.

LV stages impact points locations are not troublesome for safety. Only AVUM impact point is quite close to South America's Pacific coast, because of the constraint needed to cope with the P/L entry conditions. Nevertheless, margins are enough (few kilograms of propellant are sufficient) to envisage a powered CCAM while maintaining a large residual reserve.

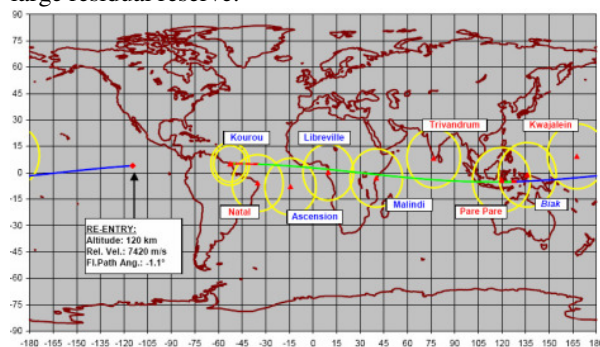


Figure 19 ORT: ascent and de-orbiting trajectory ground track

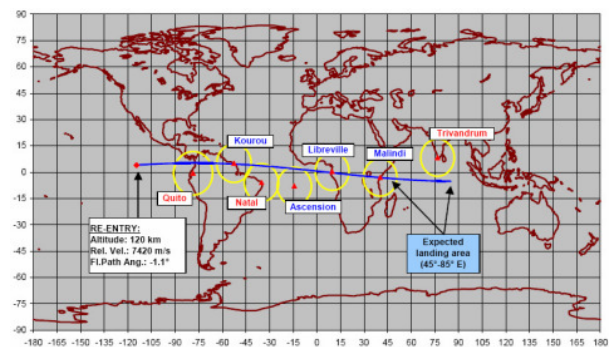


Figure 20 ORT: re-entry ground track (approximate)

B. Avum Compatibility

The ORT mission is within Vega nominal mission range, excepting for the fact that the de-orbit firing of the AVUM LPS is carried out before separating the P/L, thus originating a peculiar maneuver whose main additional features to be investigated are⁵:

- possible impacts on accuracy of guidance and navigation subsystems;
- AVUM characteristics during de-orbit modified by the presence of the P/L, influencing the controllability task;
- AVUM mass to be de-orbited increased by the P/L presence, thus increasing the propellant needs;
- AVUM P/L pointing, release, and collision avoidance maneuvers to be executed on the reentering orbit with a time constraint (before the atmospheric entry);
- additional LPS firing needed for collision avoidance (nominally performed with ACS only, due to the subsequent de-orbiting firing).

The above mentioned features are not deemed to introduce troubles, as:

- Mission duration is in line with the current baseline. For de-orbiting, the presence of the P/L w.r.t. the baseline (AVUM only de-orbitation), ensures that the acceleration during the final maneuver is lower, thus to smaller dispersions, not reducing the accuracy. Consequently, the accuracy figures provided by the user manual (i.e.: ± 10 km on perigee and apogee altitude; $\pm 0.05^\circ$ on inclination; $\pm 0.1^\circ$ on RAAN – all at 1σ) remain applicable. A preliminary computation on case #5, adopted in sect. 6 for mission analysis, show that

these errors reflects on the status at 120 km with an error on entry velocity of ~ 4.1 m/s and an error on flight path angle of $\sim 0.14^\circ$ (all at 1σ).

2. De-orbit conditions for the baseline maneuver (AVUM only de-orbitation) are the most demanding from the controllability point of view due to the backward shift of the CoM, which dramatically reduces the TVC control arm. The presence of the P/L during the maneuver eases the task by shifting the CoM forward.
3. Propellant margin is quite significant as USV mass is about half Vega capability on the required mission, thus the increased propellant need for de-orbit can be managed.
4. All the named maneuvers are designed to be performed in less than 500 s, while about 2000 s pass from the de-orbiting firing end to the arrival at the atmospheric interface (120 km), leaving enough time for their execution. Visibility aspect may be critical (TBC).
5. This feature is not critical, in terms of both feasibility (existing on the baseline Vega mission – LPS grants up to 5 re-ignitions) and available time (see point 4. above), and will be investigated if needed.

C. FTB_X Compatibility

The analysis shows the criticality of the vertical fin position, which prevent from a direct connection between USV tail fuselage section and the 937B adapter, introducing the need of a distancing device. Both nose and wing tips are well inside the fairing envelope.

Figure 21 represents the vehicle attitude scheme adopted to evaluate the need for ballast masses and the envelope compatibility with the preliminary FTB_X adapter module (length = 0.4 [m]).

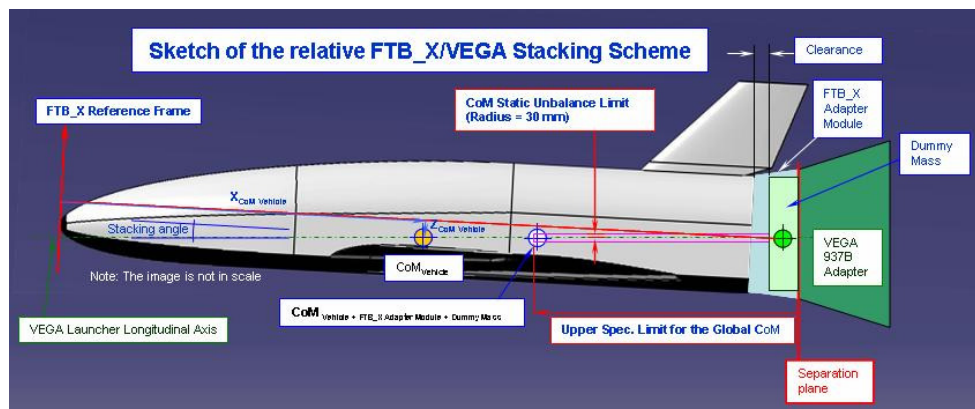


Figure 21 Sketch of the relative FTB_X/VEGA stacking scheme

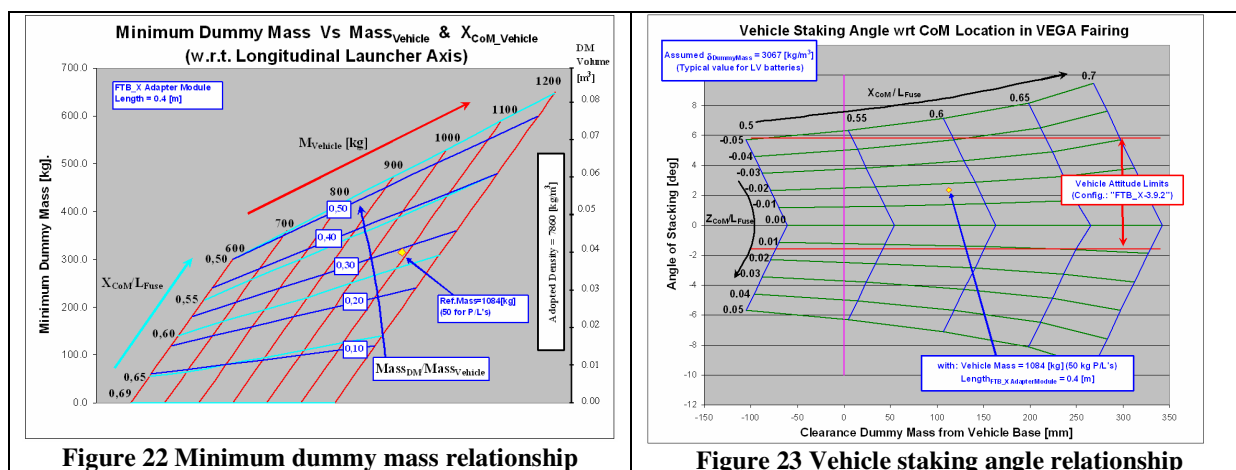
Figure 22 shows the estimated minimum dummy mass need to match VEGA launcher requirements, vs. the vehicle mass and wrt its Centre of Mass location, along X. Data are referred to a preliminary version of the FTB_X adapter module.

Figure 23 shows the possible vehicle attitude angle (stacking) able to minimize the static unbalance of the global CoM relevant to the FTB_X vehicle, including Dummy Mass and FTB_X adapter module, from the VEGA longitudinal axis, to match the launcher applicable requirements.

The estimated dummy mass is related to the VEGA fairing constraints and, in particular, appears, for the shown data ranges, that the dummy mass value is strongly related to the vehicle CoM location along the X axis, lower effects have been observed with reference to the vehicle mass variation.

It is important to underline that for the baseline configuration with Mass Vehicle = 1084 kg (including 50 kg for P/L's, with $X_{CoM}/L_{Fuse}=0.586$ and $Z_{CoM}/L_{Fuse} = -0.016$) the total dummy mass could be devoted to auxiliaries power supply batteries as well as other system device (e.g. RCS).

The preliminary analysis of the VEGA User Manual shows that there are not pre-definite requirements for spacecraft dynamic balancing that may affects the stacking setup.



The reference Payload adapter for Vega LV is the standard 937 B used also for Ariane launchers. The connection is insured by a jettisonable clamp-band fitted with jumpers.

Withdrawal is ensured by a spring-loaded push button system.

Anyway, the P/L may also provide its own customized adapter and separation system as well, which shall be compliant with the interface characteristics imposed by the LV.

VI. Safety considerations

A preliminary overview was carried out of norms and rules to be applied to the USV-X vehicle in order to allow the execution of its flight, controlling the inherent risks.

Flight safety is responsibility of the launching state⁶.

As a consequence, launches from the European space center in French Guiana are under direct responsibility of French authorities. Flight safety is managed by the Guyana Space Center (CSG), an establishment of the Centre National d'Etudes Spatiales (CNES), which is responsible for drawing up and having applied the general safety rules allowing control of the risks involved in the space activities.

For this purpose, CNES has elaborated a "safety doctrine" which is pursued in the "CSG safety regulations", a set of requirements and rules to be complied with in the field of safety by all users of Ariane launch base.

Among the general objectives of the "safety doctrine", flight safety deals with the protection of persons, property, and environment, both within and, essentially, without the launch base. This is performed by means of an iterative process ("Submission") aimed at controlling the hazards generated by the mission activities, which start at the beginning of the project design, is integrated into all project activities, and continues through to project operation. In this frame, risk identification and evaluation shall be performed on the basis of analyses which allow to undertake a risk reduction process, either by proper system design, or by suitable operation procedures.

As a general guideline at the current status of the USV program, the following principles, which are based on Vega re-entering stages analyses⁵, can be listed that may apply to early phases of design:

- ☐ overflight of populated lands shall be limited;
- ☐ landing site shall be selected in remote zones;
- ☐ de-orbiting and re-entry profile shall be selected such that in case of any anomalous
- ☐ operation, debris fall down in open sea, out of nations' Economic Exclusion Zone (EEZ) waters in order to avoid limitations to navigation⁷.

VII. Conclusion

The activities, performed during the trade-off and design phases of the FTB_X flying test bed, have been oriented to develop a concept allowing to test new technologies and alternative strategies of atmospheric re-entry, as a preparatory step for new generation space vehicles whose operation is envisaged in the long term scenario. Particular care has been devoted to make the design compatible with the use of a new generation of Ultra High Temperature Ceramics, developed with the efforts of CIRA and other Italian developers within the USV program. Further, new strategies of guidance and control will be implemented in the system, in alternative to the capabilities

of presently operational re-entry vehicles, to be confirmed by a suitable level of analysis of stability and manoeuvrability issues, both in longitudinal and in lateral, since the beginning of the design activities, as here shown.

As final consideration, it is important to remark how the concepts and technologies behind the FTB_X design are to be seen as a national asset in the future perspective of the development of a family of flying test beds, even beyond the objectives of the USV program, aimed at supporting the Italian technology and system knowledge growth, in the field of atmospheric re-entry and thus enforcing Italian positioning in the development of new generations of space planes.

Acknowledgments

The authors wish to thank Giuseppe Spaziani (CIRA) for his contribution to CAD modelling and Antonio Rinalducci (ELV) for his helpful support to the launch analysis.

References

-
- ¹ Monti R., Pezzella G., "Low Risk Re-Entry Vehicle", AIAA 12th International Space Planes and Hypersonic Systems and Technologies Conference, Norfolk, Virginia USA Dec. 2003.
 - ² Rufolo G.C., Roncioni P., Marini M., Votta R., Palazzo S. "Experimental and numerical aerodynamic data integration and aerodatabase development for the PRORA USV-FTB-1 reusable vehicle", *Proceedings of the 14th AIAA/AHI, International Space Planes and Hypersonic Systems and Technologies Conference*, Canberra (AU), AIAA-2006-8031, November 2006.
 - ³ Schettino, A., Pezzella, G., Gigliotti, M., De Matteis, P., Brach Prever E. and Massobrio, F., "Aero- Thermal Trade- Off Analysis of the Italian USV Re- Entry Flying Test Bed", *Proceedings of the 14th AIAA/AHI, International Space Planes and Hypersonic Systems and Technologies Conference*, Canberra (AU), AIAA-2006-8114, November 2006.
 - ⁴ USV-NT-1-A-0001-SYS Iss. 1 - Rev. 1, "USV_X – VEGA compatibility study", ELV, (unpublished)
 - ⁵ Vega User's Manual Iss. 3 / Rev. 0, Mar. 2006
 - ⁶ CSG Safety Regulations CSG-RS-10A-CN Ed. 5/3
 - ⁷ Convention on international liability for damage caused by space objects (appended to UN Resolution No. 2777)